Mechanistic Aspects of the Electrocatalytic Oxidative Cleavage of 1,2-Diols by Electrogenerated Pb(IV)

Frank Marken, Adam M. Squires, John A. Alden, and Richard G. Compton*

Physical and Theoretical Chemistry Laboratory, Oxford University, South Parks Road, Oxford OX1 3QZ, U.K.

Jonathan E. H. Buston and Mark G. Moloney

Dyson Perrins Laboratory, Oxford University, South Parks Road, Oxford OX1 3QY, U.K.

Received: November 14, 1997; In Final Form: December 10, 1997

The electrochemical oxidation of Pb(II) to Pb(IV) in acetonitrile solution containing benzoic acid and pyridine is possible at a basal-plane pyrolytic-graphite electrode and associated with a rapid ligand exchange at the metal center. The Pb(IV) species generated under these conditions is shown to react with diols such as 1,2:5,6-di-*O*-isopropylidene-D-mannitol, 1,2-ethanediol, *cis*- and *trans*-1,2-cyclopentanediol, which undergo a two-electron oxidation associated with carbon−carbon bond cleavage. Voltammetric data obtained by both channel flow cell and rotating disk electrode experiments are analyzed by numerical simulation. Consistent results for a second-order EC′ (electrocatalytic) reaction pathway were obtained. Voltammetric data obtained by systematically varying the concentration of pyridine and benzoic acid reveal a complex mechanism with a distinct trend in reaction rate for each diol expressed in terms of apparent fractional reaction orders when analyzed in terms of a chemically oversimplified EC′ mechanism. This behavior is given mechanistic significance by analysis of the data using numerical simulation employing the following "branched" $EC_{rev}C_{rev}C_{irrev}'$ reaction scheme, which allows all the experimental results to be rationalized (benz = benzoic acid, py = pyridine): Pb(II) $\rightleftarrows$ Pb(IV) + 2e$^-$; Pb(IV)(benz)$_h$(py)$_i$ + diol $\rightleftarrows$ Pb(IV)(benz)$_h$(diol)(py)$_i$ with rate constants k_1 and k_{-1} for the forward and reverse reactions, respectively; Pb(IV)(benz)$_{h+j}$(diol)(py)$_{i-k}$ + k(py) $\rightleftarrows$ Pb(IV)(benz)$_h$(diol)(py)$_i$ + j(benz) with rate constants k_2 and k_{-2} for the forward and reverse reactions, respectively; Pb(IV)(benz)$_h$(diol)(py)$_i$ $\rightarrow$ Pb(II) + products with rate constant k_f. Here, the chemical processes are associated with appropriate rate constants, k_n, and the equilibrium constant of a process is given by $K_n = k_n/k_{-n}$ (n = 1, 2). The "true" second-order rate constants K_1k_f obtained for the electrocatalytic cleavage of 1,2:5,6-di-*O*-isopropylidene-D-mannitol ($k = j = 1$), $K_1k_f = (36 \pm 7) \times 10^3$ M^{-1} s^{-1}, 1,2-ethanediol ($k = 1$; $j = 2$), $K_1k_f = (70 \pm 14) \times 10^3$ M^{-1} s^{-1}, *trans*-1,2-cyclopentanediol ($k = 1$; $j = 0$), $K_1k_f = (180 \pm 36) \times 10^3$ M^{-1} s^{-1}, and *cis*-1,2-cyclopentanediol ($k = j = 0$), $K_1k_f = (280 \pm 56) \times 10^3$ M^{-1} s^{-1} are similar to within 1 order of magnitude. The effect of the diffusion of coexisting species coupled via fast preequilibria to the irreversible chemical process is discussed in respect to the physical meaning of the rate constants determined by applying a simplified mechanistic scheme.

Introduction

Redox catalysts[1,2] are used for the electrochemically controlled conversion of molecules via a redox process that, in the absence of the catalyst, would only react under much more extreme conditions to yield, if at all, the same amount and type of product. The $Pb^{4+/2+}$ redox couple is an example of a reagent with a broad spectrum of stoichiometric uses in organic chemistry[3,4] especially with recent advances in synthetically useful carbon−carbon coupling processes[5−13] and for which a recycling procedure, for example by electrochemical means under mild conditions at an electrode surface, would be highly desirable.

Recently, the oxidation of 1,2-ethanediol by an in situ electrochemically generated redox catalyst Pb(IV) benzoate has been shown to be feasible at graphite electrodes and under very mild conditions in acetonitrile solution.[14] The proposed reaction pathway for this process is summarized in Scheme 1. Lead present in the form of Pb(II) benzoate is oxidized at the electrode, and the chemical reaction of Pb(IV) benzoate with the 1,2-diol closes the reaction cycle. Consistent with literature reports,[15] it was found that pyridine added as a base considerably affected the rate constant of the oxidation process, with the 1,2-ethanediol being oxidized to form formaldehyde and two protons. A rate law first order in pyridine was proposed.[14]

SCHEME 1: Mechanistic Pathway for the Electrocatalytic Oxidative Cleavage of 1,2-Diols by Pb(IV) Generated at an Electrode Surface

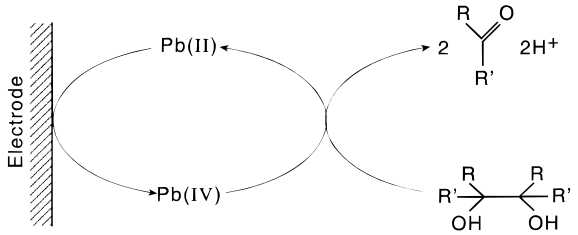

In this study a wider range of conditions and four different 1,2-diols, namely, ethanediol, 1,2:5,6-di-*O*-isopropylidene-D-

S1089-5647(98)00215-6 CCC: $15.00
Published on Web 01/27/1998

mannitol, *cis*- and *trans*-1,2-cyclopentanediol (see structures),

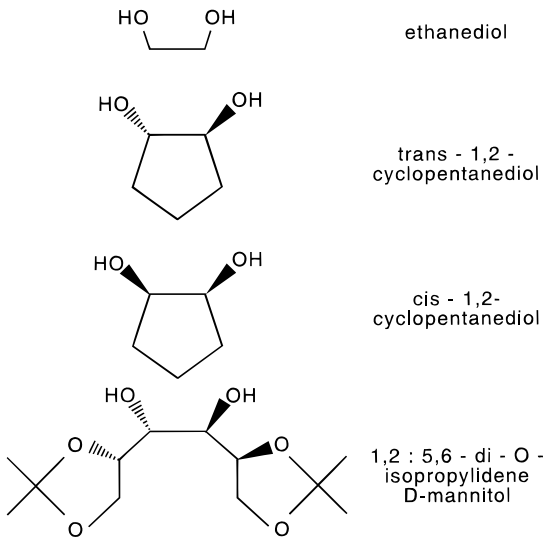

are used in order to unravel more of the details of the mechanistic scheme. In particular the effects caused by pyridine and by benzoic acid are analyzed in order to extend the scope of the electrochemical process and to allow the prediction and optimization of conditions in which the Pb(IV) reagent is more reactive.

Interpreting Complex Mechanisms Using Simplified Reaction Schemes: Deceptions and Limitations

Preequilibrium chemical steps are very common and present in many chemical processes in condensed media. These chemical steps can involve extremely fast association/dissociation reactions or isomerizations. The experimental detection of fast preequilibria is possible if intermediates are present in measurable amounts or if the experimental time scale is chosen to be fast enough to compete with the equilibration process. However, usually preequilibrium processes remain undetected and the use of a simple mechanistic scheme is sufficient in order to explain experimental data.

The following example illustrates the possible effects of a preequilibrium for the case of an electrocatalytic (EC′) type electrode process (eq 1).

$$\mathrm{A} \rightleftarrows \mathrm{B} + \mathrm{e}^- \tag{1a}$$

$$\mathrm{B} + \mathrm{X} \underset{k_{-1}}{\overset{k_1}{\rightleftharpoons}} \mathrm{C} + \mathrm{Y} \tag{1b}$$

$$\mathrm{C} \xrightarrow{k_\mathrm{f}} \mathrm{A} + \text{products} \tag{1c}$$

In this reaction scheme a redox center A is activated by electron transfer at the electrode surface and after the equilibration process (1b) undergoes an irreversible chemical step in which the starting material A is regenerated. The reagents X and Y may be present in excess, and the nature of the product species remains unspecified. The response of this reaction to variation in [X] and [Y] data for the limiting currents of rotating disk steady-state voltammetric experiments was generated numerically by employing the Digisim 2.0 software package. Limiting currents were calculated for $K_{eq} = k_1/k_{-1} = 4$, $k_f = 10\ s^{-1}$, [A] = 0.001 M, [X]/[Y] = 10^{-2}−10^2 over a range of settings for the rotation speed (10−200 rad s^{-1}) (for model parameters, see Experimental Section). The actual magnitude of the concentrations [X] and [Y] was not found to be important as long as [X] and [Y] were present in >10-fold excess over the electroactive species [A] and the preequilibrium step 1b was very fast. That is, the equilibrium (eq 1b) remains undisturbed throughout the diffusion layer and the concentrations for the species X and Y remain practically constant. Accordingly, the parameters k_1 and k_{-1} are chosen to be sufficiently large so that their values do not affect the calculated limiting currents. This corresponds to a very fast preequilibrium followed by an essentially irreversible chemical-reaction step. The analysis of the generated data is possible again by numerical simulation, although with a somewhat simpler reaction mechanism (eq 2):

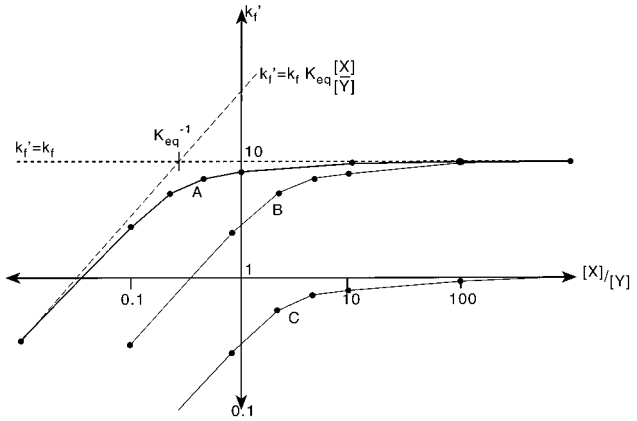

Figure 1. Plot of the rate constant k_f' in eq 2 versus the concentration ratio [X]/[Y] in eq 1 used for data generation: (A) data generated with $K_{eq} = 4$, $k_f = 10$; (B) data generated with $K_{eq} = 0.4$, $k_f = 10$; (C) data generated with $K_{eq} = 0.4$, $k_f = 1$. Dashed lines indicate the limiting cases (see text).

$$\mathrm{A} \rightleftarrows \mathrm{C}' + \mathrm{e}^- \tag{2a}$$

$$\mathrm{C}' \xrightarrow{k_\mathrm{f}'} \mathrm{A} + \text{products} \tag{2b}$$

This analysis gives a set of rate constants k_f' that now depend on the concentrations of the reagents X and Y. In Figure 1 values for the obtained rate constants plotted versus the parameter [X]/[Y] are shown (line A). As noted above, the data shown in this plot were generated by assuming the equilibrium step 1b to be extremely fast. For real chemical processes this hypothesis may rapidly break down for both very high or very low values of [X]/[Y]. Additionally, the effect of changing K_{eq} and k_f in the above mechanistic scheme (eq 1) is indicated (lines B and C). Two limiting cases at very low and at very high values for [X]/[Y] can be observed, and the corresponding rate laws may easily be extracted (see Figure 1).

$$K_{eq}\frac{[X]}{[Y]} < 1 \quad \frac{\mathrm{d[products]}}{\mathrm{d}t} = k_\mathrm{f}'[\mathrm{C}'] = k_\mathrm{f}K_{eq}\frac{[X]}{[Y]}[\mathrm{C}'] \tag{3}$$

$$K_{eq}\frac{[X]}{[Y]} > 1 \quad \frac{\mathrm{d[products]}}{\mathrm{d}t} = k_\mathrm{f}'[\mathrm{C}'] = k_\mathrm{f}[\mathrm{C}'] \tag{4}$$

For the case of a high concentration of [X] or a low concentration of [Y] a first-order dependence in both [X] and $[Y]^{-1}$ is detected and the concentration [C′] ≈ [B].

The observed rate laws (see eqs 3 and 4) only describe the limiting cases for the analysis of the reaction scheme shown in eq 1. The complete rate law for the reaction scheme analyzed

with the scheme in eq 2 may be written as

$$\frac{\mathrm{d[products]}}{\mathrm{d}t} = k_f'[C'] = k_f \frac{K_{eq}\dfrac{[X]}{[Y]}}{K_{eq}\dfrac{[X]}{[Y]} + 1}[C'] \qquad (5)$$

This expression may be derived recognizing that [B] + [C] = [C′] by comparison of eqs 1 and 2. Insertion of the equilibrium condition $K_{eq}[X]/[Y] = [C]/[B]$ before inserting $k_f'[C'] = k_f[C]$ yields eq 5. For the analysis of the complex electrode process described by eq 1 the application of the mechanistic scheme given in eq 2 can result in the observation of rather complex behavior. For very low concentration of the intermediate C the diffusion and the concentration gradient of this species may be neglected, and the rate constant so determined is consistent with the preequilibrium case (eq 3). For the case of essentially all intermediate being converted into C, the preequilibrium remains undetected (eq 4). Only for the intermediate case with two diffusing species B and C, additional information, such as the value of K_{eq}, may be obtained from the experimentally determined rate law, and an apparently fractional reaction order for the rate constant k_f' in [X] and [Y] is observed if the analysis is made in terms of a conventional rate law of the form rate = $[X]^x[Y]^y$.

The expressions become slightly more involved in the case of more than one equilibrium step. Two or more preequilibria may be coupled via a branched or a consecutive pathway. The simple treatment outlined above always may be used to predict the resulting rate law and reaction order. The following reaction scheme is similar to the one above except that two consecutive preequilibria occur.

$$A \rightleftarrows B_1 + e^- \qquad (6a)$$

$$B_1 + X \underset{k_{-1}}{\overset{k_1}{\rightleftarrows}} B_2 \qquad (6b)$$

$$B_2 \underset{k_{-2}}{\overset{k_2}{\rightleftarrows}} C + Y \qquad (6c)$$

$$C \xrightarrow{k_f} A + \text{products} \qquad (6d)$$

The rate-law expression derived by the method outlined above for this process is

$$\frac{\mathrm{d[products]}}{\mathrm{d}t} = k_f \frac{K_1K_2\dfrac{[X]}{[Y]}}{1 + K_1[X] + K_1K_2\dfrac{[X]}{[Y]}}[C'] \qquad (7)$$

In this case the reaction rate is dependent on the sequence of the preequilibria, and a change such as exchange of the reaction steps 6b and 6c gives a different result for conditions other than those for the limiting cases. As might be expected, it is possible to simplify the equations describing this more complex process by choosing $K_1[X] \ll 1$ and $K_2[Y]^{-1} \gg 1$. Under these conditions the additional intermediate B_2 can be neglected and the reaction scheme is reduced to that involving one simple preequilibrium (eq 1).

The rate law predicted in eq 7 is readily verified by a numerical simulation of the steady-state limiting currents for rotating disk voltammetry following the protocol of generating data with a full mechanistic scheme and analysis with a partial mechanistic scheme (eq 2). The effect of the second preequilibrium step is to modify the transition zone in which the apparently fractional reaction order is observed and to cause distinct reaction orders in respect to [X] and [Y].

The introduction of increasingly different diffusion coefficients for each species in the mechanistic schemes used in this section causes the simple treatment to gradually fail. For instance, a diffusion coefficient for the species B and C, which is significantly smaller than that of the other species in eq 1, will cause a less satisfactory description of the data by the simpler scheme (eq 2). What remains is an approximate tool that still allows valuable conclusions concerning an improved mechanism that can then provide the basis of a more complex numerical simulation as will be shown below.

Experimental Section

Reagents and Instrumentation. Electrolyte solutions were prepared from NBu_4PF_6 (electrochemical grade, Fluka), acetonitrile (dried and distilled, Fisons), pyridine (AnalaR, BDH), and benzoic acid (BDH). Pb(II) benzoate was prepared as reported elsewhere.[14] Ethanediol (BDH), 1,2:5,6-di-*O*-isopropylidene-D-mannitol, *cis*-1,2-cyclopentanediol, and *trans*-1,2-cyclopentanediol (all 98%, Aldrich) were used as purchased.

An Oxford Electrodes potentiostat and a Lloyd P3 recorder were used for voltammetric experiments. The electrode used for rotating disk voltammetry was a 4.94-mm diameter basal-plane pyrolytic-graphite (Le Carbone) disk electrode mounted in Teflon and for channel flow cell studies a rectangular basal-plane pyrolytic-graphite plate electrode embedded in a channel flow cell.[14] As counter electrodes, a graphite rod or a platinum gauze were used and a saturated calomel electrode (SCE) served as the reference electrode. Solutions were degassed with high-purity argon prior to measurements. Experiments were conducted at 20 ± 2 °C.

Software and Simulation. Data obtained from rotating disk electrode voltammetry was analyzed by using simulation data obtained from a Digisim 2.0 (Bioanalytical Systems) PC software package. To generate data corresponding to steady-state transport-limited currents for rotating disk voltammetry, the corresponding option and with preequilibrium disabled were selected. Model parameters were exponential grid factor β = 0.1, potential step of 0.005 V, Gauss−Newton iteration 1, $D^*/k^* = 50$, $X_{max}/[(\upsilon/w)^{1/2}(D/\upsilon)^{1/3}] = 6$, and R_o^* minimum = 20. A backward-implicit (BI) method computer program suitable for an electrode of 3 mm × 3 mm size coded in Fortran and executed on a Sun SPARC workstation was used to numerically model transport-limited currents obtained from channel flow cell experiments.[14] To simplify the numerical model describing the Pb-mediated two-electron oxidation, a one-electron process was used and the calculated limiting current multiplied by a factor 2. Fitting of kinetic parameters was achieved on a small number (typically four) of selected data points before calculating the result for the complete set of data.

To prove the nature of the reaction products to be consistent with the proposed reaction scheme, a bulk electrolysis experiment with 1,2:5,6-di-*O*-isopropylidene-D-mannitol (500 mg, 1.9 mmol) and Pb(II) $(benzoate)_2$ (45 mg, 0.1 mmol) in 100 mL of acetonitrile (0.2 M NBu_4PF_6) in a divided H-type stirred electrolysis apparatus was performed. Continuous polarization of the basal-plane pyrolytic-graphite anode (area 10 cm^2) at +1.6 V vs SCE led to the formation of brown material that gradually reduced the electrode activity because of blocking. Therefore, the potential was stepped in 1-s intervals to 0.0 V vs SCE where it was held for 0.1 s, thereby allowing the cleaning of the

electrode surface and a continuous electrolysis process. Two equivalents of charge (380 C) corresponding to an overall two-electron oxidation process workup by removal of the solvent, diethyl ether extraction, and chromatography over silica afforded 2,2-dimethyl-4-dihydroxymethyl-1,3-dioxolane as a white crystalline product (379 mg, 67% yield based on the starting material) identified by ^{1}H- and ^{13}C-NMR spectroscopy.

Results and Discussion

The oxidation of Pb(II) benzoate in acetonitrile solution[14] proceeds via a two-electron process at basal-plane pyrolytic-graphite electrodes in the presence of both excess pyridine (py) and excess benzoic acid (Hbenz) (eq 8).

$$\mathrm{Pb(II)(benz)_2} + 2(\mathrm{Hbenz}) + 2(\mathrm{py}) \rightleftarrows \mathrm{Pb(IV)(benz)_4} + 2(\mathrm{Hpy^+}) + 2\mathrm{e^-} \quad (8)$$

Although the details of the effect of benzoic acid and pyridine may be considerably complex, their known[16] protonation equilibria in acetonitrile, $pK_{a,Hpy} = 12.3$ and $pK_{a,Hbenz} = 20.7$, are consistent with a very weak buffer system with pyridine acting as a proton trap. All experiments described in this study employ a moderate to high excess of pyridine, and therefore, affects due to protons in the reaction environment can, to a first approximation, be ignored. Therefore, the notation adapted for benzoic acid, [benz], 1,2-diol, [diol], and pyridine, [py], makes no comment on their state of protonation. It is hoped that this improves the clarity of the arguments presented below.

Under the conditions described in this work the heterogeneous electron transfer process at the basal-plane pyrolytic-graphite electrode is sufficiently fast to allow the detection of a limiting current due to convective diffusion in the solution phase and therefore to allow steady-state hydrodynamic voltammetric methodology to be used in order to determine qualitative and quantitative details of the chemical reactions coupled to the $Pb^{4+/2+}$ oxidation process. Rotating disk voltammograms for the oxidation of 1 mM Pb(II) benzoate for different rotation speeds were obtained, and from the analysis of the plot of diffusion-limited current versus square root of rotation speed[17] the diffusion coefficient for Pb(II) benzoate, $D_{Pb} = (1.0 \pm 0.1) \times 10^{-9}$ m^2 s^{-1} at 20 °C, was found. In the mechanistic analysis reported below this diffusion coefficient is assumed to describe all mechanistically significant metal complexes containing Pb as a central atom. The effect of variation of the pyridine concentration from 0.01 to 0.2 M and of the benzoic acid concentration from 0.01 to 0.05 M on the diffusion coefficient D_{Pb} was found to be within the reported experimental error, and the possible change in diffusion coefficient due to diol added to the solution as a reagent was assumed to be negligible.

In the presence of aliphatic 1,2-diols, such as ethanediol, hydrodynamic voltammetry of Pb(II) benzoate in acetonitrile solution shows considerably enhanced currents consistent with a catalytic EC′ reaction[14] (Scheme 1). The Pb^{2+} species that is regenerated within the diffusion layer at the electrode surface is responsible for the significant increase in current. In Figure 2 the plot of the limiting current versus square root of rotation speed obtained at a rotating disk electrode for the oxidation of 2 mM 1,2:5,6-di-*O*-isopropylidene-D-mannitol at a 4.94-mm diameter basal-plane pyrolytic-graphite electrode in the presence of 0.01 M benzoic acid, 0.1 M pyridine, and 1 mM Pb(II) benzoate is shown. Line A corresponds to the expected limiting current in the absence of diol when only Pb^{2+} is oxidized. The analysis of the set of data points obtained in the presence of small amounts of 1,2-diols requires a numerical simulation that

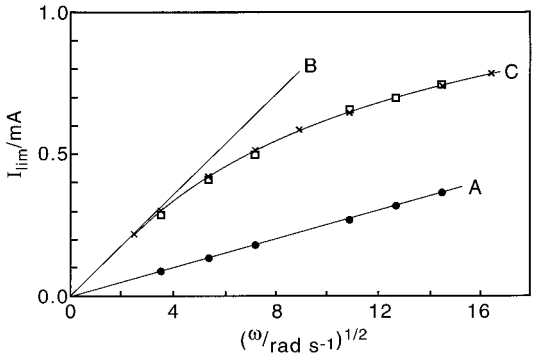

Figure 2. Plot of the limiting currents (□) observed by rotating disk electrode voltammetry for the oxidation of 1 mM Pb(II) benzoate in acetonitrile/0.1 M NBu_4PF_6 in the presence of 2 mM 1,2:5,6-di-*O*-isopropylidene-D-mannitol, 0.1 M pyridine, and 0.01 M benzoic acid: (A) limiting current in the absence of diol; (B) limiting current for diffusion-controlled limiting current; (C) limiting current obtained by numerical simulation employing the kinetic scheme given in eq 10 with $k_f' = 27\,000$ s^{-1}.

accounts for the type of transport near the electrode employed as well as the overall second-order nature of the process introduced by the low concentration of diol.

However, the implementation of these procedures requires reliable values for the diffusion coefficient of the 1,2-diols studied. The determination of the diffusion coefficients of the 1,2-diol, D_{diol}, may be based either on an approximate correlation given by Wilke and Chang[18] or on measurements that exploit conditions under which the catalytic diol oxidation proceeds effectively under full mass-transport control. In Figure 2 it can be seen that for very low diol concentration and slow rotation speed the observed limiting currents approach linear behavior. This implies that the current reflects the rate of transport of Pb plus diol to the electrode. Levich analysis for a two-electron oxidation process in this region (line B) may therefore be used to extract the value of D_{diol} directly from the corresponding limiting current $I_{lim,diol}$, which corresponds to the difference between the observed limiting current and the known contribution from the oxidation of the Pb complex.

$$I_{lim,diol} = I_{lim,total} - I_{lim,Pb} \quad (9)$$

A summary of approximate and experimental values for D_{diol} is given in Table 1. A significant variation is found for the diffusion coefficients of ethanediol. The high value calculated from the Wilke−Chang expression[18] corresponding to a small molecular volume appears to be significantly reduced possibly because of association with other species, such as pyridine or benzoate. A third approach for the determination of the diffusion coefficients can be based on a fitting procedure due to the significantly different effects caused by the second-order rate constant k_f' (see eq 10 below) and the diffusion coefficient D_{diol} on the shape of the plot of the limiting current versus the square root of rotation speed (see line C in Figure 2). However, this two-parameter fit procedure may, when applied on its own, cause wrong mechanistic assumptions in the model to be hidden. On the other hand, in case of agreement between the diffusion coefficients determined independently, the accuracy of this fitting method makes it a valuable test for the reliability of the mechanistic model. The agreement between the different approaches is satisfactory, thereby apparently corroborating the applied mechanistic model of a second-order EC′ process. For further analysis of experimentally obtained data the diffusion coefficients obtained by method iii (Table 1) were used. The

TABLE 1: Diffusion Coefficients[a] for 1,2-Diols

method	ethanediol $D_{diol}/10^{-9}$ m^2 s^{-1}	1,2:5,6-di-*O*-isopropylidene-D-mannitol $D_{diol}/10^{-9}$ m^2 s^{-1}	*cis*-1,2-cyclopentanediol $D_{diol}/10^{-9}$ m^2 s^{-1}	*trans*-1,2-cyclopentanediol $D_{diol}/10^{-9}$ m^2 s^{-1}
i[b]	3.3	1.1	1.8	1.8
ii[c]	2.2 ± 0.2	1.5 ± 0.2	2.0 ± 0.2	1.8 ± 0.2
iii[d]	1.8 ± 0.1	1.3 ± 0.1	1.6 ± 0.1	1.5 ± 0.1

[a] In acetonitrile/0.1 M NBu_4PF_6 solution containing 0.1 M pyridine and 0.01 M benzoic acid at a temperature of 20 ± 2 °C. Errors estimated. [b] Estimated by the Wilke−Chang procedure.[18] [c] Measured by extrapolation of the limiting current observed under steady-state conditions for the limit of complete oxidation of the 1,2-diol. [d] Obtained by a fitting procedure (see text).

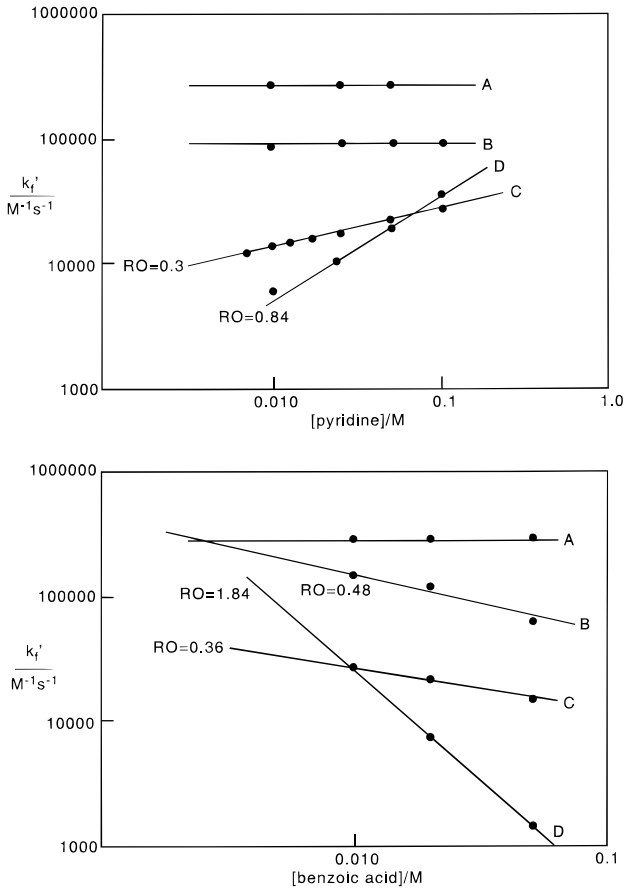

Figure 3. (a, top) Plot of the second-order rate constant k_f' obtained by applying the reaction scheme in eq 10 versus the concentration of pyridine and (b, bottom) versus the concentration of benzoic acid: (A) *cis*-1,2-cyclopentanediol; (B) *trans*-1,2-cyclopentanediol; (C) 1,2:5,6-di-*O*-isopropylidene-D-mannitol; (D) ethanediol.

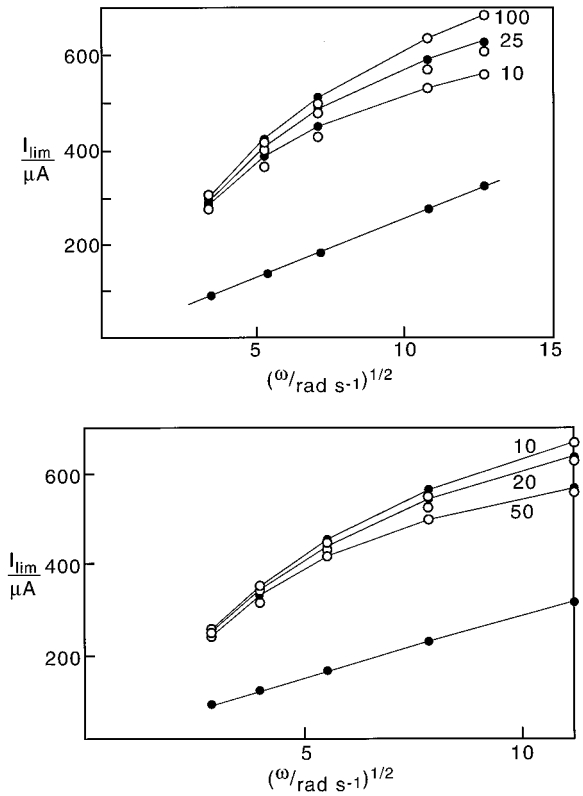

Figure 4. Plot of the calculated (●) and the experimentally observed (○) limiting currents for the electrocatalytic oxidation of 1,2:5,6-di-*O*-isopropylidene-D-mannitol at a 4.94-mm diameter basal-plane pyrolytic-graphite rotating disk electrode in acetonitrile (0.1 M NBu_4PF_6) in the presence of 1 mM Pb(II) benzoate: (a, top) 2 mM 1,2:5,6-di-*O*-isopropylidene-D-mannitol, 10 mM benzoic acid, effect of 10, 25, and 100 mM pyridine; (b, bottom) 1.2 mM 1,2:5,6-di-*O*-isopropylidene-D-mannitol, 50 mM pyridine, effect of 10, 20, and 50 mM benzoic acid.

diffusion coefficients for pyridine, 2.1×10^{-9} m^2 s^{-1}, and for benzoic acid, 1.7×10^{-9} m^2 s^{-1}, were estimated.[18]

The analysis of both data obtained from channel flow cell experiments and from rotating disk electrode experiments gave consistent results within experimental error. The following reaction scheme was used for the analysis of the measured current data.

$$A \rightleftarrows B + 2e^- \qquad (10a)$$

$$B + D \xrightarrow{k_f'} A + \text{products} \qquad (10b)$$

The rate constants k_f' were determined, but although good agreement was achieved by fitting the experimental data based on the simple mechanistic EC′ pathway, the possible effects of pyridine and benzoic acid have not yet been accounted for.

The effect of pyridine was examined for four different 1,2-diols (see structures). In each case voltammograms were obtained over a range of rotation speeds and the rate constants k_f' for the EC′ reaction scheme determined. The variation in the magnitude of these second-order rate constants is surprisingly characteristic for each of the different 1,2-diols (Figure 3). An increase in pyridine concentration appears to increase the second-order rate constant for the homogeneous oxidation of 1,2:5,6-di-*O*-isopropylidene-D-mannitol and ethanediol. In contrast, the cases of *cis*- and *trans*-1,2-cyclopentanediols concentration-independent values were detected even at very low pyridine concentrations. Complementary observations have been made for the effect of varying the concentration of benzoic acid (Figure 3b). In this case again *cis*-1,2-cyclopentanediol appears to be unaffected, whereas for the oxidation of the other three diols a *decrease* in rate with an increase of benzoic acid concentration was found. The double-logarithmic plot allows the individual reaction orders to be determined (values indicated).

Most strikingly the reaction orders determined from these measurements are of noninteger nature. The reason for this behavior must be a mechanistic scheme more complex than that

TABLE 2: Kinetic Parameters for the Electrocatalytic Oxidation of 1,2-Diols[a] Obtained by Fitting Numerical Data for the Limiting Current of Rotating Disk Electrode Voltammograms and Channel Flow Cell Voltammograms to Experimental Data

1,2-diol	K_1 M^{-1}	K_2	k_f s^{-1}	K_1k_f M^{-1} s^{-1}
1,2:5,6-di-*O*-isopropylidene-D-mannitol	200 ± 100	0.2 ± 0.04	180 ± 90	$(3.6 \pm 0.7) \times 10^4$
1,2-ethanediol	350 ± 140	$(5 \pm 1) \times 10^{-4}$ M	200 ± 100	$(7.0 \pm 1.4) \times 10^4$
trans-1,2-cyclopentanediol	90 ± 45	$(25 \pm 5) \times 10^{-4}$ M	$(2 \pm 1) \times 10^3$	$(18 \pm 3.6) \times 10^4$
cis-1,2-cyclopentanediol	10 ± 5		$(28 \pm 14) \times 10^3$	$(28 \pm 6) \times 10^4$

[a] In acetonitrile/0.1 M NBu_4PF_6 at a temperature of 20 ± 2 °C. Errors estimated.

used for analysis (eq 10). A second rate-determining reaction step could be present or, more likely, fast preequilibria may occur. The Pb(IV) metal center is known to undergo very rapid ligand exchange,[19] and in order to interpret the observed data, the effect of preequilibria on electrochemical processes[20] as outlined above may be used. A general $EC_{rev}C_{rev}C_{irrev}'$ mechanistic scheme for both types of effects caused by pyridine and caused by benzoic acid in the 1,2-diol oxidation process may be proposed.

$$\mathrm{Pb(II)} \rightleftarrows \mathrm{Pb(IV)} + 2e^- \tag{11a}$$

$$\mathrm{Pb(IV)(benz)}_h\mathrm{(py)}_i + \mathrm{diol} \underset{k_{-1}}{\overset{k_1}{\rightleftharpoons}} \mathrm{Pb(IV)(benz)}_h\mathrm{(diol)(py)}_i \tag{11b}$$

$$\mathrm{Pb(IV)(benz)}_{h+j}\mathrm{(diol)(py)}_{i-k} + k\mathrm{(py)} \underset{k_{-2}}{\overset{k_2}{\rightleftharpoons}} \mathrm{Pb(IV)(benz)}_h\mathrm{(diol)(py)}_i + j\mathrm{(benz)} \tag{11c}$$

$$\mathrm{Pb(IV)(benz)}_h\mathrm{(diol)(py)}_i \xrightarrow{k_f} \mathrm{Pb(II)} + \mathrm{products} \tag{11d}$$

In this mechanistic scheme the electrochemical production of Pb(IV) in eq 11a indicates the formation of a species of unknown ligand-sphere composition. This step is followed by fast but undetected equilibration processes that cause the formation of the dominant or "**source**" species $Pb(IV)(benz)_h(py)_i$ and $Pb(IV)(benz)_{h+j}(diol)(py)_{i-k}$. Then two fast equilibrium steps (eqs 11b and 11c) couple these metal complexes to the reacting or "**sink**" species $Pb(IV)(benz)_h(diol)(py)_i$, which in the rate-determining and irreversible chemical step (eq 11d) completes the catalytic cycle. On the basis of the arguments given above, all further preequilibrium steps necessary to convert Pb(IV) into the desired intermediate can be ignored. The intermediates that can be "seen" by the electrochemical measurement are those that contribute to the diffusion process and have nonnegligible concentrations in the reaction layer. Further, a branched, nonconsecutive preequilibrium has been chosen (eqs 11b and 11c) in order to avoid the complication of determining the appropriate reaction sequence and to keep the mechanistic model as close as possible to the anticipated system of ligand-exchange equilibria at the Pb metal center. Although other complex mechanistic schemes might be employed to fit the experimental data, the scheme in eq 11 has the advantage of being relatively simple and chemically plausible. With known stochiometric factors j and k, the three parameters K_1, K_2, and k_f are the only unknowns. Values of these have been obtained by optimization, minimizing the variance between experimental data and numerically generated data for the model mechanism.

In the case of the oxidation of 1,2:5,6-di-*O*-isopropylidene-D-mannitol the preequilibrium in eq 11c has to be written with $j = k = 1$ corresponding to the exchange of one equivalent of each benzoic acid and pyridine. The expected rate law may be derived approximately (ignoring unequal diffusion effects and the fact that there is no excess in the concentration of diol):

$$\frac{\mathrm{d[products]}}{\mathrm{d}t} = k_f \frac{1}{1 + \frac{1}{K_1}\frac{1}{[\mathrm{diol}]} + \frac{1}{K_2}\frac{[\mathrm{benz}]}{[\mathrm{py}]}}[\mathrm{Pb(IV)}] \tag{12}$$

Numerical simulation of data from rotating disk voltammetric experiments by employing Digisim 2.0 for the full reaction scheme (eq 11) was possible for $j = k = 1$, and in Figure 4 experimental and numerical data points are shown to fit satisfactorily with $K_1 = 200$ M^{-1}, $K_2 = 0.2$, and $k_f = 180$ s^{-1}. Data are summarized in Table 2. The estimated error from the fitting procedure is rather large for K_1 and k_f. However, their product K_1k_f remains constant and is therefore well defined. This is in agreement with the second-order nature of the process, which allows reliable analysis only for the second-order rate constant. A further illustration of this effect follows below.

In the case of the catalytic oxidation of *cis*-1,2-cyclopentanediol no change in the second-order rate constant k_f' is observed for variation of both the benzoic acid and pyridine concentrations. The proposed mechanistic scheme (eq 11) may be applied for the case $j = k = 0$. Only one preequilibrium is introduced in order to describe the complexation reaction between Pb(IV) complex and the diol. However, the fitting procedure allows only the product, K_1k_f, to be determined reliably. In Table 2 it can be seen that this product must correspond to the value of k_f'.

In the case of the oxidation of *trans*-1,2-cyclopentanediol only a weak benzoic acid dependence with an apparent reaction order of 0.48 (Figure 3b) was detected. Therefore, an expression with $j = 0$ and $k = 1$ can be used.

$$\frac{\mathrm{d[products]}}{\mathrm{d}t} = k_f \frac{1}{1 + \frac{1}{K_1}\frac{1}{[\mathrm{diol}]} + \frac{1}{K_2}[\mathrm{benz}]}[\mathrm{Pb(IV)}] \tag{13}$$

The determination of the three kinetic parameters via fitting yields $K_1 = 90$ M^{-1}, $K_2 = 0.0025$ M, and $k_f = 2000$ s^{-1} (Figure 5). Again, the product K_1k_f is determined reliably (see Table 2).

The voltammetric data obtained for the oxidation of 1,2-ethanediol suggest an apparent reaction order of ca. 1 in pyridine and ca. 2 in benzoic acid. Therefore, the equilibrium step 11c is chosen with $j = 1$ and $k = 2$. Correspondingly, the following expression can be derived for the idealized case of identical diffusion coefficients and excess diol.

$$\frac{\mathrm{d[products]}}{\mathrm{d}t} = k_f \frac{1}{1 + \frac{1}{K_1}\frac{1}{[\mathrm{diol}]} + \frac{1}{K_2}\frac{[\mathrm{benz}]^2}{[\mathrm{py}]}}[\mathrm{Pb(IV)}] \tag{14}$$

The loss of two equivalents of benzoate ligands from the Pb complex for the conversion of the "source" species to the reacting or "sink" species is remarkable and possibly due to the sterically nondemanding and flexible ligand characteristics of ethanediol. Here, the loss of a benzoate ligand is very likely to be associated with the loss of a proton, for example, from

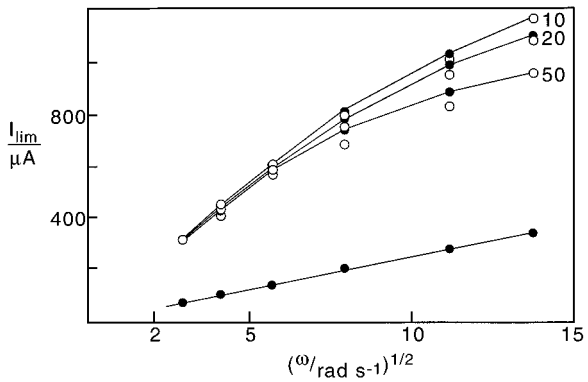

Figure 5. Plot of the calculated (●) and the experimentally observed (○) limiting currents for the electrocatalytic oxidation of 2 mM *trans*-1,2-cyclopentanediol at a 4.94-mm diameter basal-plane pyrolytic-graphite rotating disk electrode in acetonitrile (0.1 M NBu_4PF_6) in the presence of 1 mM Pb(II) benzoate, 50 mM pyridine, and of 10, 20, and 50 mM benzoic acid.

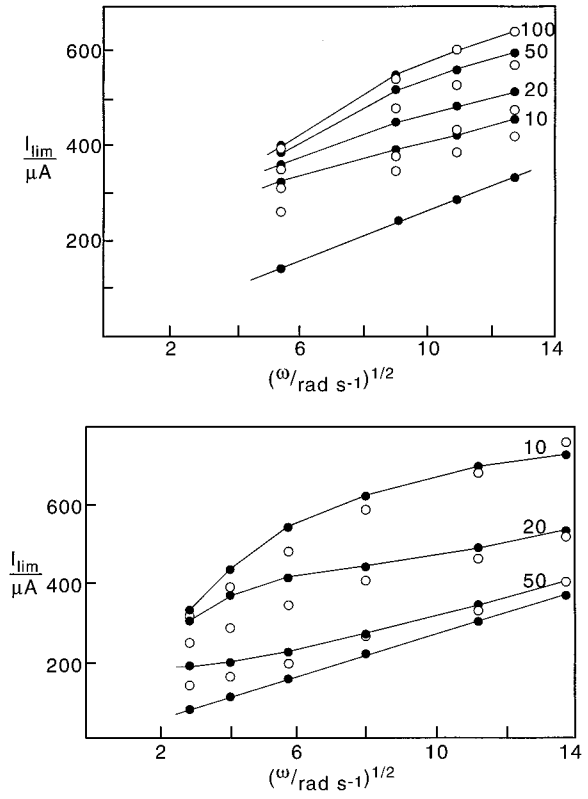

Figure 6. Plot of the calculated (●) and the experimentally observed (○) limiting currents for the electrocatalytic oxidation of ethanediol at a 4.94-mm diameter basal-plane pyrolytic-graphite rotating disk electrode in acetonitrile (0.1 M NBu_4PF_6) in the presence of 1 mM Pb(II) benzoate: (a, top) 1.2 mM ethanediol, 10 mM benzoic acid, effect of 10, 20, 50, and 100 nM pyridine; (b, bottom) 2 mM ethanediol, 50 mM pyridine, effect of 10, 20, and 50 mM benzoic acid.

the coordinated diol. The overall charge of the Pb complex is thereby kept constant.

Problems in the fitting were encountered, and numerical data obtained for $K_1 = 350\ M^{-1}$, $K_2 = 0.0005$ M, and $k_f = 200\ s^{-1}$ are shown to result only in a poor fit of the experimental data in Figure 6. Deviations are pronounced at low rotation speeds and at low concentrations of benzoic acid. A possible reason for this complication is the fact that a rather complex sequence of preequilibria involving two equivalents of benzoic acid and pyridine occur and the rate for the overall process will be below that of the slowest step of a particular sequence. This could violate the condition of an extremely fast preequilibrium, and as a result, a mismatch of experimental and numerical data depending on the rate of mass transport occurs. However, the use of a more complex mechanistic model appears to be unwarranted for the limited data set presented in this study.

Conclusions

Kinetic parameters for the Pb(IV)-mediated electrocatalytic oxidation of four 1,2-diols have been obtained from steady-state voltammetric methods. A mechanistic model based on rapid preequilibria successfully explains the effects caused by pyridine and benzoic acid present in the reaction mixture and allows the dissection of a "true" second-order rate constant K_1k_f. The agreement of the data obtained for different diols (Table 2) suggests a common mechanistic pathway and only a small effect of structural features of the diols such as trans or cis configuration on the rate of the carbon−carbon bond scission. However, structural features of the diols appear to be very important in modifying the ligand sphere of the intermediate Pb(IV) metal complex, thereby shifting the sensitive preequilibria for this highly fluxional system.

Acknowledgment. The EPSRC (Grant No. GR/1693167) is acknowledged for providing financial support, and we thank Dr. Thies Thiemann for valuable discussions. F.M. thanks the Royal Society for the award of a University Research Fellowship and J.A.A. Keble College for a senior studentship.

References and Notes

(1) For a review see the following. Simonet, J. In *Organic Electrochemistry*; Lund, H., Baizer, M. M., Eds.; Marcel Dekker: New York, 1991; p 1217.

(2) Steckhan, E. *Top. Curr. Chem.* **1987**, *142*, 1.

(3) See, for example, the following. (a) Rubottom, G. M. In *Oxidation in Organic Chemistry*; Trahanovsky, W. H., Ed.; Academic Press: London, 1982; Chapter 1, Part D. (b) Mihailovic, M. L.; Cekovic, Z.; Lorenc, L. In *Organic Syntheses by Oxidation with Metal Compounds*; Mijs, W. J., De Jonge, C. R. H. I., Eds.; Plenum Press: London, 1986; p 741.

(4) Sheldon, R. A.; Kochi, J. K. *Org. React. (N.Y.)* **1972**, *19*, 279.

(5) Pinhey, J. T. *Aust. J. Chem.* **1991**, *44*, 1353.

(6) Moloney, M. G.; Thompson, R. M.; Wright, E. *Main Group Met. Chem.* **1996**, *19*, 133.

(7) Pinhey, J. T. *Pure Appl. Chem.* **1996**, *68*, 819.

(8) Morgan, J.; Pinhey, J. T. *Tetrahedron Lett.* **1994**, *35*, 9625.

(9) Parkinson, C. J.; Hambley, T. W.; Pinhey, J. T. *J. Chem. Soc., Perkin Trans. 1* **1997**, 1465.

(10) Koen, M. J.; Morgan, J.; Pinhey, J. T.; Sherry, C. J. *J. Chem. Soc., Perkin Trans. 1* **1997**, 487.

(11) Morgan, J.; Pinhey, J. T.; Rowe, B. A. *J. Chem. Soc., Perkin Trans. 1* **1997**, 1005.

(12) Morgan, J.; Pinhey, J. T.; Sherry, C. J. *J. Chem. Soc., Perkin Trans. 1* **1997**, 613.

(13) Morgan, J.; Hambley, T. W.; Pinhey, J. T. *J. Chem. Soc., Perkin Trans. 1* **1996**, 2173.

(14) Marken, F.; Leslie, W. M.; Compton, R. G.; Moloney, M. G.; Sanders, E.; Davies, S. G.; Bull, S. D. *J. Electroanal. Chem.* **1997**, *424*, 25.

(15) See, for example, the following. Goldschmid, H. R.; Perlin, A. S. *Can. J. Chem.* **1960**, *38*, 2280.

(16) Izutsu, K. *Acid-Base Dissociation Constants in Dipolar Aprotic Solvents*; Blackwell: Oxford, 1990.

(17) See, for example, the following. Rieger, P. H. *Electrochemistry*, 2nd ed.; Chapman & Hall: London, 1994.

(18) Wilke, C. R.; Chang, P. *AIChE J.* **1955**, *1*, 264.

(19) Buston, J. E. H.; Claridge, T. D. W.; Moloney, M. G. *J. Chem. Soc., Perkin Trans. 2* **1995**, 639.

(20) See, for example, the following. Schmickler, W. *Interfacial Electrochemistry*; Oxford University Press: Oxford, 1996; p 145.